III International Conference on Particle-based Methods – Fundamentals and Applications
PARTICLES 2013
M. Bischoff, E. Oñate, D.R.J. Owen, E. Ramm & P. Wriggers (Eds)

NUMERICAL SIMULATION OF BUOYANCY DRIVEN DROPLET RISING UNDER INFLUENCE OF AN ELECTRICAL FIELD USING ISPH

N. Tofighi, A. Rahmat and M. Yildiz

Faculty of Engineering and Natural Sciences
Sabanci University, Istanbul, 34956, Turkey
nima@sabanciuniv.edu

Key words: Incompressible Smoothed Particle Hydrodynamics, Multiphase Flows, Droplet Deformation, Electro Hydrodynamics, Leaky Dielectric Model

Abstract. In this study, a method for modeling incompressible, immiscible two phase fluid flows influenced by an external electrical field in the context of incompressible smoothed particle hydrodynamics in two dimensions has been described. Continuum surface force model is employed while leaky dielectric model is used to incorporate the effects of electrical field on fluid flow. The proposed method is employed to numerically simulate buoyancy driven rising motion of a single droplet in quiescent fluid influenced by an electrical field.

1 Introduction

The motion of a droplet under the effect of gravitational force where two fluids of different properties have interfacial contact surfaces is one of the most common features observed in many engineering and natural processes and have been a subject of interest for modeling in many computational fluid dynamics (CFD) studies. Analytical solutions are available for simplified cases of buoyancy driven flow while a vast number of numerical studies employing different methods have been conducted on different test cases [1, 2]. Controlling the dynamics of the lighter fluid interface is of special interest and introducing an electric field provides a mechanism to influence the body force otherwise dominated by gravity. In such cases, use of electrical forces may potentially benefit convective transport and mixing in many technical applications [3].

In this study, a two dimensional incompressible smoothed particle hydrodynamics (ISPH) scheme based on the projection method proposed by Cummins and Rudmann [4] is developed to simulate buoyancy driven flows under the influence of an electrical field. Surface tension forces are taken into consideration using Continuum Surface Force (CSF) model [5] while a leaky dielectric model is opted to include forces exerted due to the presence of electric field [6]. In order to asses the capability of the proposed method, rising of a droplet under the effect of gravity and an electrical field in a quiescent fluid has been studied for different electrical Bond numbers. Results obtained show that electrical field has considerable effect on the evolution of bubble while rising.

2 Mathematical Formulation

Equations governing an incompressible flow may be written as

$$\nabla \cdot \mathbf{u} = 0, \tag{1}$$

$$\rho \frac{\mathrm{D}\mathbf{u}}{\mathrm{D}t} = -\nabla p + \nabla \cdot \boldsymbol{\tau} + \mathbf{f}_{(b)} + \mathbf{f}_{(s)} + \mathbf{f}_{(e)}, \tag{2}$$

where $\mathbf{u}$ is the velocity vector, p is pressure, ρ is density, t is time, δ is Dirac delta function and $\mathrm{D}/\mathrm{D}t = \partial/\partial t + u^k \partial/\partial x^k$ represents the material time derivative. Here, $\boldsymbol{\tau}$ and $\mathbf{f}_{(b)}$ are viscous stress tensor and body forces exerted on the flow, respectively. While body force is taken to be $\rho\mathbf{g}$, where $\mathbf{g}$ is gravitational acceleration, viscous stress tensor is defined as

$$\boldsymbol{\tau} = \mu \left(\nabla \mathbf{u} + (\nabla \mathbf{u})^T \right), \tag{3}$$

where μ denotes viscosity and superscript T represents the transpose operation. For the sake of computational simplicity and efficiency, local surface tension force is expressed as an equivalent volumetric force according to the CSF method originally proposed by Brackbill *et al.* [5],

$$\mathbf{f}_{(s)} = \sigma \kappa \hat{\mathbf{n}} \delta. \tag{4}$$

Here, surface tension coefficient, σ, is taken to be constant while κ represents interface curvature, $-\nabla \cdot \hat{\mathbf{n}}$, where $\hat{\mathbf{n}}$ is unit surface normal vector. To be able to distinguish between different phases, a color function $\hat{c}$ is defined such that it assumes a value of zero for one phase and unity for the other. Interface curvature, unit normals and surface tension forces related to each phase are computed using its corresponding color function and will be discussed further in the following paragraphs.

Following the same mindset (as of surface tension forces) for electrical forces, electric stress is calculated by taking the divergence of the Maxwell stress tensor [6]. Taking the incompressibility of the flow into account, volumetric electric force may be written as

$$\mathbf{f}_{(e)} = -\frac{1}{2} \mathbf{E} \cdot \mathbf{E} \nabla \varepsilon + q \mathbf{E}. \tag{5}$$

Here, $\mathbf{E}$, ε and q represent electric field, permittivity and volume charge density near interface. Disregarding any time-varying magnetic field and assuming that the flow conforms to leaky dielectric conditions, *i.e.* electric relaxation time is much shorter than viscous timescale, an electric potential ϕ may be defined as

$$\nabla \cdot (\gamma \nabla \phi) = 0, \tag{6}$$

where γ is the electrical conductivity. Upon solving for ϕ, $\mathbf{E}$ and q are defined as

$$\mathbf{E} = -\nabla\phi, \tag{7}$$

$$q = \nabla \cdot (\varepsilon\mathbf{E}). \tag{8}$$

Interactions between SPH particles are facilitated through an interpolation function $W(r_{\mathrm{ij}}, h)$ where r_{ij} is the magnitude of distance vector $\mathbf{r}_{\mathrm{ij}} = \mathbf{r}_{\mathrm{i}} - \mathbf{r}_{\mathrm{j}}$ between particle of interest i and its neighboring particles j while h is the smoothing length. Defining $\psi_{\mathrm{i}} = \sum_{\mathrm{j}} W_{\mathrm{ij}}$, One may smooth out the color function as $c_{\mathrm{i}} = \sum_{\mathrm{j}} \hat{c} W_{\mathrm{ij}}/\psi_{\mathrm{i}}$ which may serve to smoothen the sharp gradients in properties that may potentially destabilize the numerical method using a weighted averaging scheme over all phases, $f_{\mathrm{i}} = \sum_{\alpha=1}^{3} f_{\mathrm{i}}^{\alpha} c_{\mathrm{i}}^{\alpha}$ where f may represent density, viscosity, conductivity or permittivity, where applicable. It is also utilized to evaluate $\delta \simeq |\nabla c|$, $\kappa = -\nabla \cdot \hat{\mathbf{n}}$ and $\hat{\mathbf{n}} = \nabla c/|\nabla c|$ in (4). However, a constraint has to be enforced to keep possible erroneous normals, as pointed out by Morris [7]. In this study, only gradient values excessing a certain threshold, $|\nabla c_{\mathbf{i}}| \simeq \beta/h$, are used in surface tension force calculations. A β value of 0.08 has been found to provide accurate results without removing too much detail.

A predictor-correcter scheme is employed to advance the governing equations of flow in time using a first-order Euler approach with variable timestep according to Courant-Friedrichs-Lewy condition, $\Delta t = C_{CFL} h/u_{max}$, where u_{max} is the largest particle velocity magnitude and C_{CFL} is taken to be equal to 0.25. In predictor step all the variables are advanced to their intermediate form using following relations,

$$\mathbf{r}_{\mathrm{i}}^{*} = \mathbf{r}_{\mathrm{i}}^{(n)} + \mathbf{u}_{\mathrm{i}}^{(n)}\Delta t + \boldsymbol{\delta}\mathbf{r}_{\mathrm{i}}^{(n)}, \tag{9}$$

$$\mathbf{u}_{\mathrm{i}}^{*} = \mathbf{u}_{\mathrm{i}}^{(n)} + \left(\nabla \cdot \boldsymbol{\tau}_{\mathrm{i}} + \mathbf{f}_{(b)\mathrm{i}} + \mathbf{f}_{(s)\mathrm{i}} + \mathbf{f}_{(e)\mathrm{i}}\right)^{(n)} \Delta t, \tag{10}$$

$$\psi_{\mathrm{i}}^{*} = \psi_{\mathrm{i}}^{(n)} - \Delta t \psi_{\mathrm{i}}^{(n)} \left(\nabla \cdot \mathbf{u}_{\mathrm{i}}^{*}\right), \tag{11}$$

where starred variables represent intermediate values and superscript (n) denotes values at the n^{th} time step. Artificial particle displacement vector in (9), $\boldsymbol{\delta}\mathbf{r}_{\mathrm{i}}$, is defined as stated in [8] where a constant value of 0.06 is used.

Using intermediate values, pressure at the next time step is found by solving the Poisson equation which is then followed by corrections in position and velocity of the particles, completing the temporal transition.

$$\nabla \cdot \left(\frac{1}{\rho_{\mathrm{i}}^{*}} \nabla p_{\mathrm{i}}^{(n+1)}\right) = \frac{\nabla \cdot \mathbf{u}_{\mathrm{i}}^{*}}{\Delta t}, \tag{12}$$

$$\mathbf{u}_{\mathrm{i}}^{(n+1)} = \mathbf{u}_{\mathrm{i}}^{*} - \frac{1}{\rho_{\mathrm{i}}} \nabla p_{\mathrm{i}}^{(n+1)} \Delta t, \tag{13}$$

$$\mathbf{r}_{\mathrm{i}}^{(n+1)} = \mathbf{r}_{\mathrm{i}}^{(n)} + \frac{1}{2}\left(\mathbf{u}_{\mathrm{i}}^{(n)} + \mathbf{u}_{\mathrm{i}}^{(n+1)}\right) \Delta t + \boldsymbol{\delta}\mathbf{r}_{\mathrm{i}}^{(n)}. \tag{14}$$

However, in order to be able to handle larger density ratios between different phases of the flow, an alternative form of RHS of (13) is considered by substituting $\nabla p/\rho$ with its equivalent form, $\nabla(p/\rho) - p\nabla(1/\rho)$.

Boundary conditions are enforced through MBT method described in [9] while first derivative and Laplace operator are approximated through following expressions

$$\frac{\partial f_{\mathrm{i}}^m}{\partial x_{\mathrm{i}}^k} a_{\mathrm{i}}^{kl} = \sum_{\mathrm{j}} \frac{1}{\psi_{\mathrm{j}}} \left(f_{\mathrm{j}}^m - f_{\mathrm{i}}^m\right) \frac{\partial W_{\mathrm{ij}}}{\partial x_{\mathrm{i}}^l}, \tag{15}$$

$$\frac{\partial^2 f_{\mathrm{i}}^m}{\partial x_{\mathrm{i}}^k \partial x_{\mathrm{i}}^k} a_{\mathrm{i}}^{ml} = 8 \sum_{\mathrm{j}} \frac{1}{\psi_{\mathrm{j}}} \left(f_{\mathrm{i}}^m - f_{\mathrm{j}}^m\right) \frac{r_{\mathrm{ij}}^m}{r_{\mathrm{ij}}^2} \frac{\partial W_{\mathrm{ij}}}{\partial x_{\mathrm{i}}^l}. \tag{16}$$

Here, $a_{\mathrm{i}}^{kl} = \sum_{\mathrm{j}} \frac{r_{\mathrm{ij}}^k}{\psi_{\mathrm{j}}} \frac{\partial W_{\mathrm{ij}}}{\partial x_{\mathrm{i}}^l}$ is a corrective second rank tensor that eliminates particle inconsistencies. Left hand side of (12) is discretized as

$$\frac{\partial^2 f_{\mathrm{i}}^m}{\partial x_{\mathrm{i}}^k \partial x_{\mathrm{i}}^k} \left(2 + a_{\mathrm{i}}^{kk}\right) = 8 \sum_{\mathrm{j}} \frac{1}{\psi_{\mathrm{j}}} \left(f_{\mathrm{i}}^m - f_{\mathrm{j}}^m\right) \frac{r_{\mathrm{ij}}^k}{r_{\mathrm{ij}}^2} \frac{\partial W_{\mathrm{ij}}}{\partial x_{\mathrm{i}}^k}. \tag{17}$$

3 Simulation Results

In this section, the results for numerical simulation of a single droplet rising in a quiescent background fluid under buoyancy effects subject to an electrical field is presented. This study combines previously validated studies that were conducted separately on buoyancy driven droplet rising [8] and droplet deformation due to suspension in an external electrical field [10]. Computational domain is consisted of a 6×10 rectangle discretized with 120×200 particles placed in uniform spacing. The initial droplet is placed two radius R lengths above bottom boundary and allowed to rise in vertical direction. Non dimensional parameters controlling the evolution are

$$\mathrm{Re} = \frac{\rho_b \sigma R}{\mu_b^2}, \tag{18}$$

$$\mathrm{Bo^g} = \frac{\rho_b g R^2}{\sigma}, \tag{19}$$

$$\mathrm{Bo^e} = \frac{\varepsilon_b E_{inf}^2 R}{\sigma}, \tag{20}$$

along with ratios of droplet properties to outer fluid properties where subscripts d and b indicate droplet and background fluid, respectively. Simulations are conducted for $\mathrm{Re} = 200$, $\mathrm{Bo^g} = 4$, $\rho_d/\rho_b = \mu_d/\mu_b = \varepsilon_d/\varepsilon_b = 0.2$ and $\gamma_d/\gamma_b = 2$ while $\mathrm{Bo^e}$ is varied from 0 to 4 with unit increments.

Figure 1 provides the position of center of mass of the droplet versus time ($t^* = t\sigma R/\mu_b$) for all test cases for the duration of simulation. It is observable that electrical field

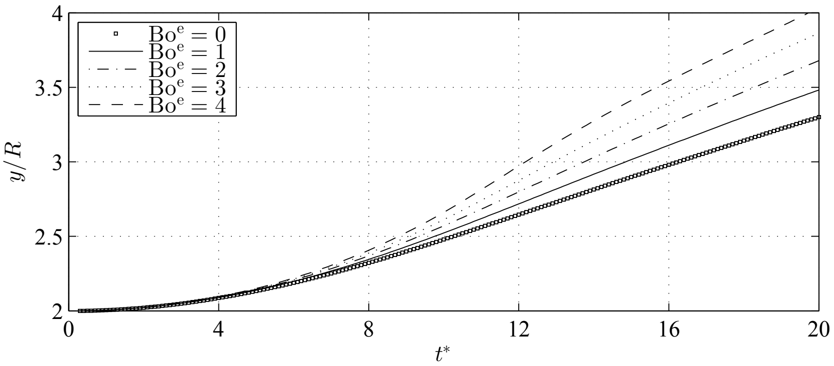

Figure 1: Position of droplet center of mass versus time for all cases.

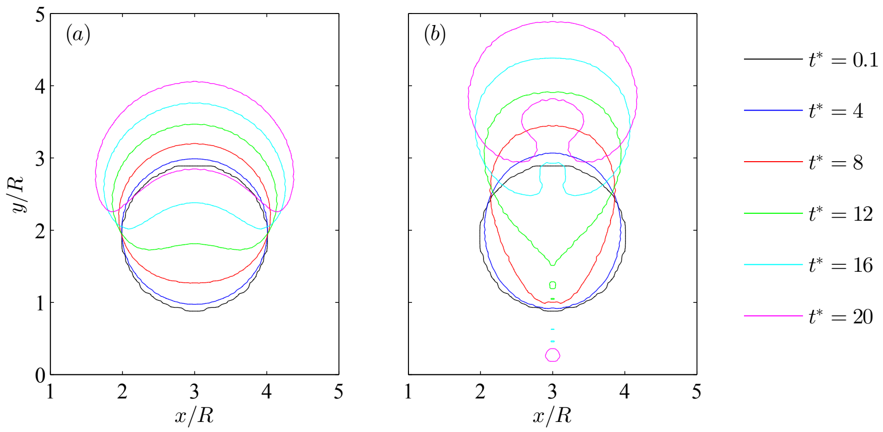

Figure 2: Time snapshots of droplet evolution (0.5 level contour of color function); (a) $\mathrm{Bo^e} = 0$, (b) $\mathrm{Bo^e} = 4$.

augments the rising motion of the droplet. Figure 2 provides time snapshots of droplet rising for cases with $\mathrm{Bo^e}$ numbers of 0 and 4. As it is seen, the presence of electric field affects the shape of the droplet in a profound manner. When no electric field is present, the droplet evolves through a series of profiles under the influence of buoyancy and surface tension forces. This results in a mushroom shaped final profile which has a wide frontal area, resulting in large drag force thus hindering the vertical motion of the droplet. However, when influenced by the electrical forces, a teardrop shape is obtained ($t^* = 8$ in fig. 2-c) which greatly reduces drag, resulting in a faster rise which is then followed by a break up at later times. It is notable that even at the later times compared to the case with no electrical field, the reduced frontal area augments the rising action of the droplet within background fluid.

These effects may be further examined if relative effect of surface tension and electrical field are compared. In order to facilitate this matter, figs. 3 and 4 provide detailed force plots of cases $\mathrm{Bo^e} = 0$ and $\mathrm{Bo^e} = 4$. In these figures, forces are scaled with the largest magnitude among both surface tension and electrical forces and relative magnitude is shown by filled contour plots while arrows provide the direction toward which the force is applied. When no electrical field is present, the droplet is only affected by surface tension and buoyancy forces. As droplet starts its vertical motion, surface tension tends to conserve the shape of the droplet in its circular form. This trend continues at later simulation times when a cavity starts to form underneath the droplet. The deformation is opposed by surface tension forces directed away from the droplet. At final stages of simulation, surface tension becomes concentrated at surface regions of high curvature which start to form at the corners. It is worth to note that along with the change in surface tension force direction, this leads to break off at higher $\mathrm{Bo^g}$ numbers which were previously studied [8]. When the same droplet is placed within the electrical field, it will experience a completely different force make up. Unlike surface tension force which always acts normal to the interface, electrical force is comprised of two parts, polarization stresses and interactions between electric charges and electric field, first and second term on the right hand side of equation 5. Polarization stresses act normal to the surface while interaction between electric charges and electric field brings up forces acting along the electric field itself. Combination of these two components brings about a complex force which tends to lengthen the droplet in vertical direction, reducing its frontal area. Darker colored contours in fig. 4 a-d comply with this observation. A break up at later times of simulation results in the droplet curving inside (fig. 4 e-f).

4 Conclusion

In this study, a two dimensional ISPH method for modeling incompressible, immiscible two phase fluid flows influenced by an external electric field has been developed. Surface tension force is exerted by implementing CSF method while leaky dielectric model is used to incorporate forces on the interface due to the presence of an electrical field. Combining previously studied cases of buoyancy driven droplet rising and droplet deformation under electrical forces, a case of buoyancy driven droplet rising affected by presence of an external electrical field has been studied numerically. Results show that the presence of an electrical field has profound effect on the shapes assumed by the droplet during its course. Set of parameters used during this study augmented rising velocity as the electrical field became stronger by reducing the frontal area and providing a more slender intermediate shape.

5 Acknowledgments

The authors gratefully acknowledge financial support provided by the Scientific and Technological Research Council of Turkey (TUBITAK) for the project 110M547 and the European Commission Research Directorate General under Marie Curie International Reintegration Grant program with the grant agreement number of PIRG03-GA-2008-231048.

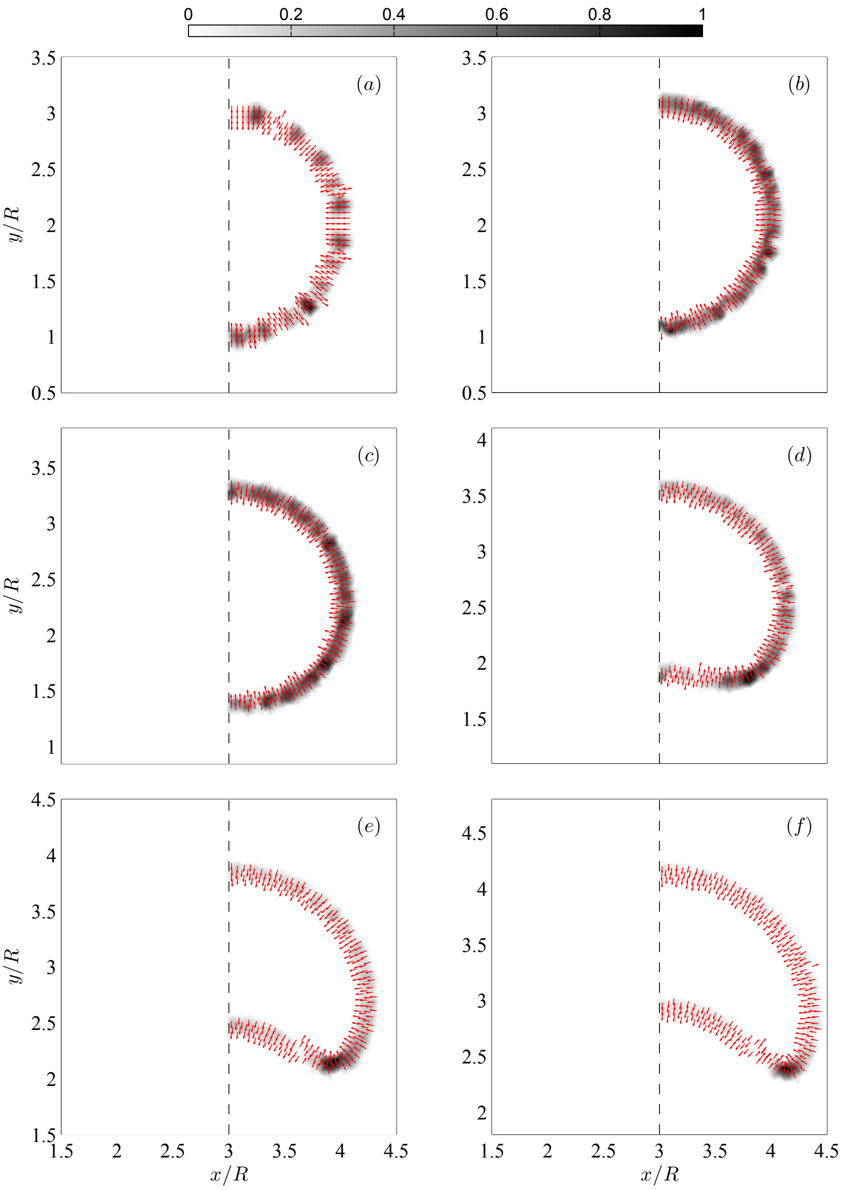

Figure 3: Force distribution for case $\mathrm{Bo}^{\mathrm{e}} = 0$; All forces are normalized with respect to maximum of both types; Arrows provide direction while contours show magnitude; At times (a) $t^* = 0.1$, (b) $t^* = 4$, (c) $t^* = 8$, (d) $t^* = 12$, (e) $t^* = 16$, (f) $t^* = 20$.

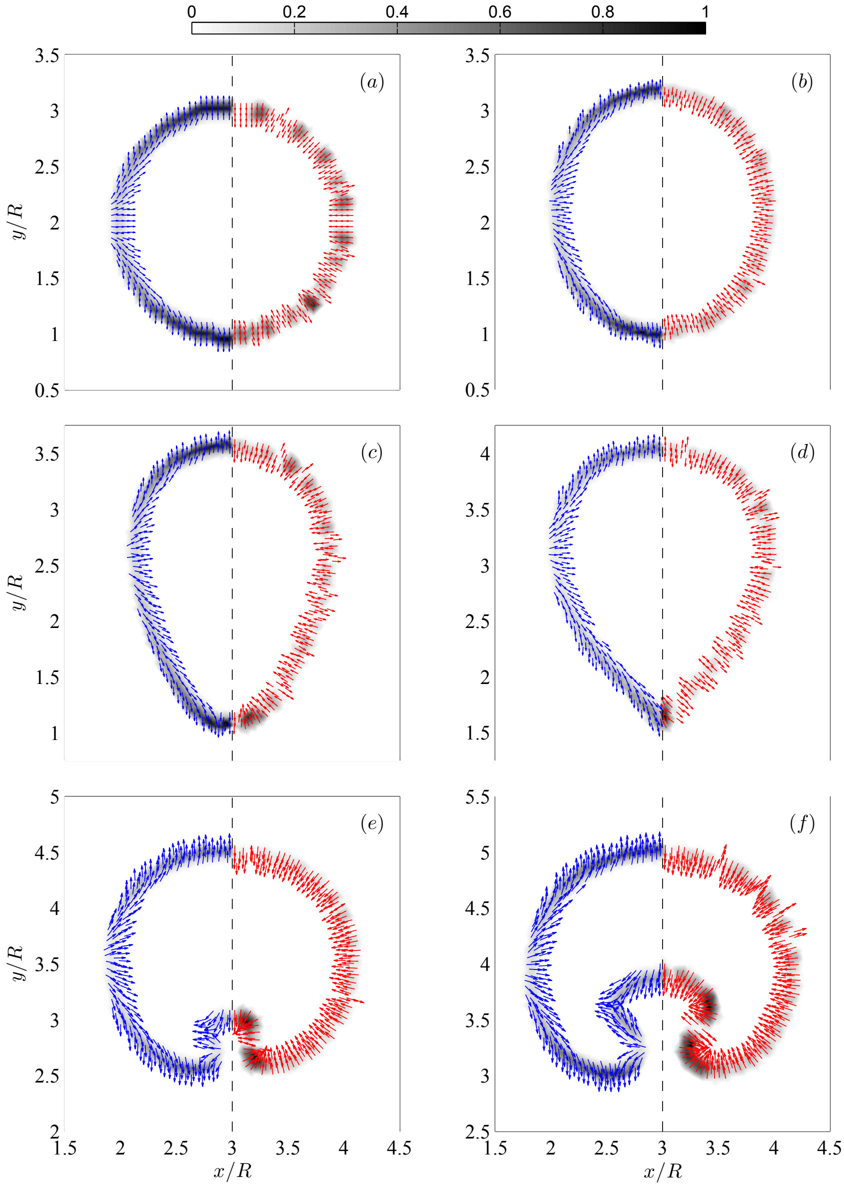

Figure 4: Force distribution for case $\mathrm{Bo}^{\mathrm{e}} = 4$; (left side) Electrical forces, (right side) Surface tension forces; All forces are normalized with respect to maximum of both types; Arrows provide direction while contours show magnitude; At times (a) $t^* = 0.1$, (b) $t^* = 4$, (c) $t^* = 8$, (d) $t^* = 12$, (e) $t^* = 16$, (f) $t^* = 20$.

References

[1] Sussman, M., Almgren, A., Bell, J., Colella, P., Howell, L. and Welcome, M. An adaptive level set approach for incompressible two-phase flows. *J. Comput. Phys.* (1999) **148**:81-124.

[2] Grenier, N., Antuono, M., Colagrossi, A., Le Touzé, D. and Alessandrini, B. An Hamiltonian interface SPH formulation for multi-fluid and free surface flows. *J. Comput. Phys.* (2009) **228**:8380-8393.

[3] Jones, T. Electrohydrodynamically enhanced heat transfer in liquids - A review. *Advances in Heat Transfer.* (1978) **14**:107-148.

[4] Cummins, S. and Rudman, M. An SPH projection method. *J. Comput. Phys.* (1999) **152**:584-607.

[5] Brackbill, J., Kothe, D. and Zemach, C. A continuum method for modeling surface-tension. *J. Comput. Phys.* (1992) **100**:335-354.

[6] Hua, J., Lim, L. and Wang, C. Numerical simulation of deformation/motion of a drop suspended in viscous liquids under influence of steady electric fields. *Phys. Fluids* (2008) **20**:113302-16.

[7] Morris, J.P. Simulating surface tension with smoothed particle hydrodynamics. *Int. J. Numer. Methods Fluids* (2000) **33**:333-353.

[8] Zainali, A., Tofighi, N., Shadloo, M.S. and Yildiz, M. Numerical investigation of Newtonian and non-Newtonian multiphase flows using ISPH method. *Comput. Methods Appl. Mech. Engrg.* (2013) **254**:99-113.

[9] Yildiz, M., Rook, R.A. and Suleman, A. SPH with the multiple boundary tangent method. *Int. J. Numer. Methods Eng.* (2009) **77**:1416-1438.

[10] Shadloo, M.S., Rahmat, A. and Yildiz, M. A smoothed particle hydrodynamics study on the electrohydrodynamic deformation of a droplet suspended in a neutrally buoyant Newtonian fluid. *Comput. Mech.* (2013):1-15.